References and Notes

1. P. K. Chapman, L. S. Pinsky, R. E. Benson, T. F. Budinger, in *Proceedings of the National Symposium on Natural and Manmade Radiation in Space*, E. A. Warman, Ed. (NASA-TM X-2440, National Aeronautics and Space Administration, Washington, D.C., 1972), p. 1002.
2. G. G. Fazio, J. V. Jelley, W. N. Charman, *Nature* **228**, 260 (1971); R. Madey and P. J. McNulty, in *Proceedings of the National Symposium on Natural and Manmade Radiation in Space*, E. A. Warman, Ed. (NASA-TM X-2440, National Aeronautics and Space Administration, Washington, D.C., 1972), p. 757.
3. P. J. McNulty and R. Madey, in *ibid.*, p. 767.
4. I. R. McAulay, *Nature* **232**, 241 (1971).
5. J. H. Fremlin, *New Sci.* **47**, 42 (1970); W. N. Charman, J. A. Dennis, G. G. Fazio, J. V. Jelley, *Nature* **230**, 522 (1971); C. A. Tobias, T. F. Budinger, J. T. Lyman, *ibid.*, p. 596; T. F. Budinger, H. Bischel, C. A. Tobias, *Science* **172**, 868 (1971).
6. C. A. Tobias, T. F. Budinger, J. T. Lyman, in *Proceedings of the National Symposium on Natural and Manmade Radiation in Space*, E. A. Warman, Ed. (NASA-TM X-2440, National Aeronautics and Space Administration, Washington, D.C., 1972), p. 416.
7. T. F. Budinger, J. T. Lyman, C. A. Tobias, *Report No. 529* (Lawrence Berkeley Laboratory, Berkeley, Calif., 1971).
8. F. J. D'Arcy and N. A. Porter, *Nature* **196**, 1013 (1962).
9. W. N. Charman and C. M. Rowlands, *ibid.* **232**, 574 (1971).
10. P. J. McNulty, *ibid.* **234**, 110 (1971); *Report No. 71-0377* (Air Force Cambridge Research Laboratories, Cambridge, Mass., 1971).

11. Supported in part by NASA grant T-111813, Air Force Cambridge Research Laboratories grant F19628-72-C-0209, and the Fannie E. Rippel Foundation. We thank J. Fennimore, F. Homan, M. Isaila, the staff of the Princeton Particle Accelerator, and H. Powsner for their help in this experiment.

* Present address: Biology Department, Brookhaven National Laboratory, Upton, N.Y. 11973.
† Present address: Lawrence Berkeley Laboratory, Berkeley, Calif. 94720.
‡ Present address: General Electric Research and Development Center, Schenectady, N.Y. 12305.

20 July 1972

Cracks and Pores: A Closer Look

Abstract. *Most pores and some cracks in several rocks, as directly viewed with a new technique, have a shape that suggests an origin early in the history of these rocks. Thus, behavior in the laboratory may be a reliable indication of behavior in the earth's crust, for electrical resistivity, permeability, or other properties that depend on microporosity.*

Nearly all rocks, even dense, crystalline varieties such as granite, diabase, or dunite, contain cavities. Although in crystalline rocks this void space may amount to less than 1 percent by volume, many physical properties are dramatically affected. This was first recognized by Adams and Williamson (*1*), who suggested that tiny cracklike voids in granite increased its compressibility severalfold. The role played by cracks and more nearly equant voids termed pores was later related quantitatively to elastic, thermal, electrical, and other properties (*2, 3*). In virtually all of these studies, a simple physical model was assumed, namely, a solid matrix with a dilute concentration of isolated cavities of circular or elliptical cross section. From this model, crack or pore parameters were calculated by using observed physical properties. For example, the pressure required to eliminate cracks gave an estimate of crack aspect ratio (*2*); the tensile strength or the low-pressure compressibility gave an estimate of crack length (*2*).

In spite of this rather extensive theoretical work on the effects of microporosity, only in rare cases have theoretical and actual crack and pore parameters been compared (*2, 4*). Direct observation of cracks and pores is difficult, partly because of their small size. In addition, in order to view pristine material in the interior of a rock sample, one has to prepare a section; to date, this has been the standard thin section or polished section (*5*). During the preparation of a section, new cracks and other surface damage are inevitable. Because of this, actual mapping of the microporosity has enjoyed little success, and parameters like crack shape, length, density, and connectivity have, we feel, never been unambiguously determined.

In the technique which we have developed for looking at the microporosity, a specimen suitable for examination with either an optical microscope or a scanning electron microscope (SEM) is obtained. The procedure is in two steps: first, the preparation of a finely ground surface (*6*), and second, removal by ion thinning (*7*) of the damage left by grinding. Vacuum evaporation of 100 to 400 Å of a metal on the rock surface renders detail visible in either a reflecting optical microscope or an SEM. With the latter, cavities and other features down to about 200 Å may be discernible (*8*).

Features typically seen at the boundary of two feldspar grains in Westerly granite (*4*) are shown in Fig. 1. The grain boundary extends from lower left to upper right in the photograph and is marked by a series of slots and irregular cavities. The feldspar grains themselves contain many small, more or less equant cavities 0.5 to about 2 μm in size; it is not known whether these cavities are tubular or more nearly spherical. Near point *a* in Fig. 1 continuous bridges of material cross a long slot; such bridged slots are common in Westerly granite. At *b* a crack is seen with one sharp and one blunt end; its length is about 30 μm and its opening at mid-length is 0.5 μm. The aspect ratio is therefore about 60. Near *c* a crack of irregular (dumbbell) shape is seen; the ends here are rounded, although a sharp-ended crack runs a short distance from one end. The aspect ratio of the crack near *c* is about 100, and that of the whole feature is about 120.

Details near the boundary of quartz and feldspar grains in Rutland quartzite (*4*) are shown in Fig. 2. In many aspects the microporosity is strikingly different from that of Westerly granite, although feldspar grains in both are riddled with tiny equant cavities about a micrometer in size (near *a* in Fig. 2). The boundary in the quartzite (which runs diagonally through *b*) is marked by a fairly continuous system of fine cracks. They are much smaller than in the granite, although the aspect ratios seem comparable; near *b*, the length is 5 to 10 μm and the aspect ratio about 100. Tiny pores of triangular cross section (they appear black in Fig. 2) intersect the cracks above and to the right of *b*. The large oval features in Fig. 2 are topographic and apparently result from the ion thinning.

We have, to date, examined three sections of Westerly granite (taken from two different blocks) and a section each of Rutland quartzite, Maryland diabase (*4*), and Mt. Albert peridotite (*9*). Observations for these rocks can be summarized as follows:

1) Grain boundaries are preferred sites for cracklike cavities, although cracks also occur within grains of biotite and feldspar, and infrequently within quartz. The grain boundary features are typically blunt-ended, are often bridged by thin septa, and occasionally show features which might be attributed to "healing" or late crystallization.

2) Cavities whose cross section is equant, or of low aspect ratio, are abundant both within feldspar (microcline, plagioclase) and at grain boundaries. Within feldspar they seem to occur randomly, whereas at grain boundaries they form rows and may alternate with slots and cracklike openings. It is not known whether equant

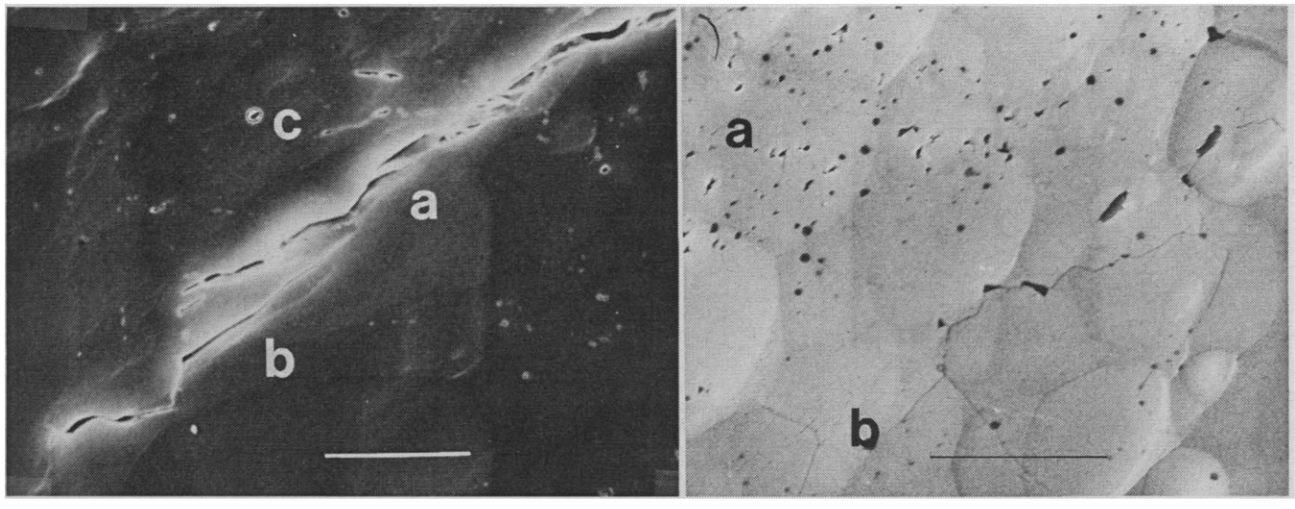

Fig. 1 (left). Photomicrograph of the boundary of two feldspar grains in Westerly granite. Cavities in this photograph have a black interior and white edges. The irregular gray areas are gentle topographic depressions which appeared after ion thinning. The white bar at the bottom is 25 μm long. Fig. 2 (right). Photomicrograph of a feldspar-quartz grain boundary in Rutland quartzite. The boundary here is marked by the series of fine cracklike cavities that appear black in this photograph. The black triangular features which intersect the cracks are cavities of unknown extent normal to the section. The black bar is 20 μm long. See text for further discussion.

cavities are isolated, or represent the emergence of long tubelike openings.

3) The porosity, as observed directly with the SEM for four rocks, is approximately in accord with the total porosity as measured by immersion and with the crack porosity as determined by elastic measurements under pressure (*4*). Thus, Westerly granite as seen with the aid of the SEM has abundant cavities with both high and low aspect ratios, whereas the diabase and peridotite have little of either. Crack porosity in the quartzite, although on a smaller scale than in the granite, exceeds pore porosity, as predicted.

4) The length of cracklike cavities is smaller than has been predicted. These cavities are almost never larger than about a tenth of the grain diameter. Intersection of more than two such cavities is uncommon, at least as viewed in a plane section.

5) For the majority of the cracklike cavities, sharp ends are the exception rather than the rule. Rarely, sharp cracks continue a short distance from the ends of long slots; more commonly, slots end abruptly, separated from one another by an uncracked bridge of material.

The above observations give rise to a number of questions: Will other granites and quartzites show the same kind of details of microporosity as Westerly granite and Rutland quartzite? How do the various cavities seen in Figs. 1 and 2 continue in the third dimension? Will quantitative measurements of the densities and shapes of the cracks and pores bear out the qualitative estimates given above? And, finally, are some of the features seen above in any way due to the sectioning procedure we use; in other words, are we really seeing the cracks and pores as they exist, undisturbed, in the interior of rock?

The last question can be commented on here. One argument that surface damage has been largely eliminated may be based on the preservation of delicate features, such as the thin bridges which span some of the longer slots in granite (Fig. 1), or the tiny scallops seen at pore edges, or the minute crystallites which appear at high magnification just inside pore edges. Additional evidence is the virtual absence of cracks in the diabase and peridotite, except near the edge of the sample, where ion thinning did not remove cracks introduced during coring. The ion bombardment itself erodes at a rate that depends on the particular mineral, but it does not seem to accentuate grain boundaries, cracks, and other macroscopic flaws.

If we are, in fact, viewing the undisturbed microporosity of typical crystalline rocks, then several important conclusions are possible. Based on their shape, hardly any of the pores and, with the exception of the quartzite, only some of the cracklike cavities appear to be of purely brittle origin. The bulk of the microporosity in our rocks, therefore, cannot have formed solely from thermal stress or by relief of pressure. These and other purely brittle processes, which must be important during the late history of typical metamorphic and igneous rocks, have frequently been suggested as an important source of the microporosity (*1, 10*). If these are not the primary causes, then most of the microporosity must be associated with the early history of these rocks. It has, therefore, been present throughout much of the period of burial in the earth's crust. Many elastic, electrical, thermal, and transport phenomena in rocks are strongly influenced by cracks and pores. To obtain the true characteristics of rock in situ, it is necessary that laboratory measurements be made on material with the same crack and pore porosity. Our results suggest that most pores and some of the cracks in laboratory samples will also be present in the crust.

Electrical conduction and other phenomena dependent on effective pressure require a continuous network of pore space. Without the detailed view of pores that is now available, it has been unclear whether the pores inferred from, say, conduction under high confining pressure might not be introduced during sampling or preparation of laboratory specimens. The pore shape (Figs. 1 and 2) would seem to rule this out. Thus, our study suggests that effects requiring the presence of pores may be reliably inferred from laboratory experiments.

W. F. Brace
E. Silver
K. Hadley
C. Goetze

Department of Earth and Planetary Sciences, Massachusetts Institute of Technology, Cambridge 02139

References and Notes

1. L. H. Adams and E. D. Williamson, *J. Franklin Inst.* **195**, 475 (1923).
2. J. B. Walsh and W. F. Brace, *Felsmechanik Ingenieurgeol.* **4**, 283 (1966).
3. J. B. Walsh and E. R. Decker, *J. Geophys. Res.* **71**, 3053 (1966); W. F. Brace, J. B. Walsh, W. T. Frangos, *ibid.* **73**, 2225 (1968).
4. W. F. Brace, *ibid.* **70**, 391 (1965).
5. W. R. Wawersik and W. F. Brace, *Felsmechanik Ingenieurgeol.* **3**, 61 (1971); H. Koide and K. Hoshino, *Jishin* **20**, 85 (1967); R. J. Willard and J. R. McWilliams, *Int. J. Rock Mech. Min. Sci.* **6**, 1 (1969); A. Timur, W. B. Hempkins, R. M. Weinbrandt, *J. Geophys. Res.* **76**, 4932 (1971); S. Baldridge and G. Simmons, *Eos* **52**, 342 (1971).
6. Grinding of a surface follows a procedure similar to that for preparation of a polished section. We used the following sizes of SiC or Al_2O_3 abrasive in the order shown: 130, 57, 30, 14, 8, and 1 μm.
7. After grinding, a specimen was placed in a Commonwealth Scientific ion milling instrument. An ionized argon beam (6 kv) bombarded the sample at an angle of 15° to 17°, knocking off individual atoms. The maximum intensity was 50 μa/mm^2. From 10 to 50 μm of material was removed from the ground surface by this bombardment. A somewhat uneven surface resulted, because thinning rates vary significantly from mineral to mineral. For example, quartz thinned approximately 10 times as fast as magnesian olivine. For granites, thinning times from 12 to 48 hours have produced satisfactory results. If thinning was continued too long, then relief was so great that detail was lost.
8. A JEOL model JSM-U3 scanning electron microscope was used to obtain magnifications of up to × 10,000. The secondary electron yield, which is sensitive to the topography of the surface and the voltage of the incident beam, was used to determine the image. The accelerating voltage was 25 kv.
9. W. F. Brace and A. S. Orange, *J. Geophys. Res.* **73**, 5407 (1968).
10. F. Birch, *ibid.* **66**, 2199 (1961); W. F. Brace and J. D. Byerlee, *Failure and Breakage of Rock* (American Institute of Mining, New York, 1967), p. 58; A. Nur and G. Simmons, *Int. J. Rock Mech. Min. Sci.* **7**, 307 (1970).

11. Supported by NSF grant GA-18342. D. Kohlstedt assisted us in sample preparation, and discussion of the results with T. R. Madden, J. B. Walsh, S. Baldridge, and P. Y. Robin was particularly helpful.

7 July 1972

Human Blood Monocytes: Stimulators of Granulocyte and Mononuclear Colony Formation in vitro

Abstract. *Human blood monocytes in a feeder layer or by use for conditioning medium produced a colony-stimulating factor capable of stimulating the in vitro growth of colonies of granulocytes and mononuclear cells from human and murine marrow. Lymphocytes and neutrophils did not stimulate colony formation, and medium conditioned by neutrophils was inhibitory. This suggests that the monocyte may control granulocyte proliferation and maturation.*

Colonies of granulocytes and mononuclear cells can be grown in vitro from the blood and marrow of animals (*1–3*) and man (*4–8*) in the presence of a colony-stimulating factor (CSF). Stimulation of colony growth can be achieved by various cell feeder layers (*1, 2, 4*), serums (*9, 10*), urine (*11*), and by conditioned medium prepared from various tissues (*12, 13*). Partial purification of CSF obtained from human urine (*14*) and mouse fibroblasts (*15*) reveals that it is a glycoprotein with a molecular weight of approximately 45,000.

Human blood leukocytes, either in a feeder layer (*4*) or by conditioning medium (*12*), will stimulate the growth of colonies from animal sources and at the present time are the best source of stimulation for growth of human colonies. However, it has not been determined which specific blood leukocyte is responsible for producing CSF. While it has been suggested that the neutrophil may be the source of CSF (*4*), this particular cell has also been reported to be inhibitory to colony growth (*16, 17*). The results of this study indicate that the blood monocyte is the cell responsible for CSF production and for the stimulation of granulocyte and mononuclear cell growth in vitro.

Eighty milliliters of blood, kept from coagulating with ethylenediaminetetraacetate was obtained by venipuncture from a healthy young adult and separated into a number of leukocyte fractions as follows.

Fraction 1: Mixed leukocytes and platelets. A sample of blood was mixed with one-fifth volume of 5 percent dextran-40 and allowed to sediment at room temperature for 1 hour. The supernatant, which was rich in leukocytes and platelets, was removed and washed three times with Seligmann's buffered salt solution (SBSS) (*18*).

Fraction 2: Mixed leukocytes without platelets. A sample of blood was defibrinated with glass beads for 30 minutes at room temperature and then handled in a manner identical to that used for fraction 1.

Fraction 3: Mononuclear cells and platelets. From another sample of blood, mononuclear cells were isolated by Ficoll-Hypaque density gradient separation (*19*). The mixture of mononuclear leukocytes and platelets was then washed three times with SBSS.

Fraction 4: Pure monocytes. A sample of cells from fraction 3 was passed through a sucrose gradient (*19*) in order to separate the mononuclear cells. The platelet-free mononuclear cells were then incubated in a concentration of 5×10^6 cells in 35-mm plastic tissue-culture dishes (Falcon Plastics) for 2 hours to allow the attachment of monocytes. Dishes were then washed vigorously with SBSS to remove nonadherent lymphocytes. Cells in one dish were stained with supravital stain to determine the leukocyte differential. The cell layer was then lysed with 1*N* NaOH and analyzed for DNA (*20*) to determine the number of cells in the monocyte monolayer.

Fraction 5: Lymphocytes. A sample of blood was incubated in 5 percent dextran containing iron particles to remove the phagocytic cells (*21*). The cells were then separated by the Ficoll-Hypaque gradient and processed as described above.

Fraction 6: Neutrophils. The neutrophils and red cells that passed through the Ficoll-Hypaque gradient in the preparation of fraction 3 were resuspended in SBSS containing 1 percent dextran. After sedimentation for 1 hour at room temperature the neutrophil-rich supernatant was washed three times with SBSS.

The differential count of each leuko-

Table 1. Ability of blood leukocytes to produce colony-stimulating factor.

Leukocyte fraction*	Differential leukocyte count†					Colonies‡
	Neutrophil	Lymphocyte	Monocyte	Eosinophil	Basophil	
1) Leukocytes with platelets	51.4	32.6	8.8	7.0	0.2	23 ± 2.8
2) Leukocytes	41.6	50.0	6.0	2.4		20 ± 4.0
3) Mononuclear cells	7.0	58.0	33.0		2.0	24 ± 3.2
4) Monocytes	2.0		98.0			35 ± 2.8
5) Lymphocytes		96.0	1.0		3.0	7.0 ± 1.2
6) Neutrophils	90.0	1.0		9.0		5.5 ± 2.4
None (control)						5.2 ± 1.6

* Fractions used to condition medium; 0.5×10^6 cells were incubated with each milliliter of medium for all fractions except 4, which contained 0.3×10^6 cells per milliliter. † Percentage of each cell type based on a differential of 500 cells. ‡ Number per 10^5 mouse marrow cells, mean ± standard error of three to five plates stimulated by 0.1 ml of conditioned medium.